

Crystal and magnetic structures of $(\text{La}_{0.70}\text{Ca}_{0.30})(\text{Cr}_y\text{Mn}_{1-y})\text{O}_3$: A neutron powder diffraction study

L. Capogna,¹ A. Martinelli,² M. G. Francesconi,³ P. G. Radaelli,⁴ J. Rodriguez Carvajal,⁵ O. Cabeza,⁶ M. Ferretti,^{2,7} C. Castellano,² T. Corridoni,⁸ and N. Pompeo⁸

¹INFM-CNR SOFT, OGG 6 Rue J. Horowitz, 38042 Grenoble, France

²INFM-LAMIA-CNR, Corso Perrone 24, 16152 Genova, Italy

³Department of Chemistry, The University of Hull, Cottingham Road, Kingston upon Hull HU6 7RX, United Kingdom

⁴ISIS Facility, Rutherford Appleton Laboratory, Chilton, Didcot, Oxfordshire OX11 0QX, United Kingdom

⁵Institut Laue Langevin, 6 Rue J. Horowitz, 38042 Grenoble, France

⁶Departamento de Física, Facultad de Ciencias, Universidad da Coruña, Campus da Zapateira s/n, 15071 A Coruña, Spain

⁷Dipartimento di Chimica e Chimica Industriale, Università di Genova, Via Dodecaneso 31, 16146 Genova, Italy

⁸Dipartimento di Fisica "E. Amaldi," Università degli Studi "Roma Tre," via della Vasca Navale, 84 I-00146 Roma, Italy

(Received 25 October 2007; revised manuscript received 28 January 2008; published 27 March 2008)

The crystal and magnetic structures of $(\text{La}_{0.70}\text{Ca}_{0.30})(\text{Cr}_y\text{Mn}_{1-y})\text{O}_3$ for $y=0.70, 0.50,$ and 0.15 have been investigated using neutron powder diffraction. The three samples crystallize in the $Pnma$ space group at both 290 and 5 K and exhibit different magnetic structures at low temperature. In $(\text{La}_{0.70}\text{Ca}_{0.30})(\text{Cr}_{0.70}\text{Mn}_{0.30})\text{O}_3$, antiferromagnetic order with a propagation vector $k=0$ sets in. The magnetic structure is G_x , i.e., of G type with spins parallel to the a axis. On the basis of our Rietveld refinement and the available magnetization data, we speculate that only Cr^{3+} spins order, whereas Mn^{4+} act as random magnetic impurities. In $(\text{La}_{0.70}\text{Ca}_{0.30})(\text{Cr}_{0.50}\text{Mn}_{0.50})\text{O}_3$ the spin order is still of the type G_x , although the net magnetic moment is smaller. No evidence for magnetic order of the Mn ions is observed. Finally, in $(\text{La}_{0.70}\text{Ca}_{0.30})(\text{Cr}_{0.15}\text{Mn}_{0.85})\text{O}_3$ a ferromagnetic ordering of the Mn spins takes place, whereas the Cr^{3+} ions act as random magnetic impurities with randomly oriented spins.

DOI: 10.1103/PhysRevB.77.104438

PACS number(s): 75.47.Lx, 75.25.+z, 75.30.Et

I. INTRODUCTION

Oxides based on the different hettotype structures, produced by cation displacement or octahedral tilting from the ideal (aristotype) ABO_3 perovskite structure, are extremely interesting materials. Their properties strongly depend on the cation located at the B site, which is a transition metal whereas A is a trivalent rare earth. One of the most extensively studied perovskites, the calcium hole-doped manganites $(\text{La}_{1-x}\text{Ca}_x)\text{MnO}_3$, shows a rich phase diagram, which is characterized by several striking structural and physical properties, such as charge, orbital and spin ordering, as well as colossal magnetoresistance,¹⁻³ all depending on the $[\text{Mn}^{3+}]/[\text{Mn}^{4+}]$ ratio at the B site.

For calcium doping concentration $0.2 < x < 0.5$ in $(\text{La}_{1-x}\text{Ca}_x)\text{MnO}_3$, two main mechanisms are at work and in competition with each other: on the one hand the double-exchange (DE) interaction favors the e_g electron delocalization between Mn^{3+} and Mn^{4+} ions in the presence of a ferromagnetic (FM) order of their t_{2g} spin cores. On the other hand, a strong electron-phonon coupling arising from the Jahn-Teller (JT) distortion of the $\text{Mn}^{3+}\text{-O}_6$ octahedra⁴ tends to localize the electrons.

Substituting Cr for Mn in $(\text{La}_{1-x}\text{Ca}_x)\text{MnO}_3$ could modulate this competition.^{5,6} It is indeed expected that Cr, by assuming the form of Cr^{3+} , hinders the JT distortions, thanks to its external electronic configuration t_{2g}^3 , which is the same as that of Mn^{4+} . Moreover, one would expect a participation of Cr^{3+} to DE. This is suggested by the effect of Cr substitution in $\text{Pr}_{0.5}\text{Ca}_{0.5}\text{MnO}_3$, which destroys the antiferromagnetism (AFM), the charge, and the orbital ordering in the Mn sublattice, favoring ferromagnetism.⁷

However, macroscopic investigations based on magnetization and resistivity measurements on $(\text{La}_{0.70}\text{Ca}_{0.30})(\text{Cr}_y\text{Mn}_{1-y})\text{O}_3$ have suggested that Cr^{3+} , despite its external electronic configuration, is not involved in the DE.^{5,6}

In this paper we tackle these issues from a microscopic point of view by studying the nuclear and the magnetic structures of $(\text{La}_{0.70}\text{Ca}_{0.30})(\text{Cr}_y\text{Mn}_{1-y})\text{O}_3$ ($y=0.70, 0.50, 0.15$) with neutron powder diffraction.

II. EXPERIMENT

The powder samples were prepared by a standard solid state reaction in air. Stoichiometric amounts of MnO_2 , La_2O_3 , CaCO_3 , and Cr_2O_3 were intimately mixed together, pelletized, and heated at 1473 K for 12 h. The mixtures were then reground and reheated at 1543 K for further 24 h. The resulting products were characterized by x-ray powder diffraction (Cu $K\alpha$ radiation, Siemens D5000).

Magnetization measurements were carried using a vibrating sample magnetometer; details are reported in Refs. 5 and 6.

Neutron powder diffraction (NPD) data were collected on the high resolution powder diffractometer D2B at the Institut Laue Langevin, Grenoble, France, using a wavelength $\lambda = 1.5940$ Å. A standard orange cryostat was used to lower the temperature to 5 K, well below the magnetic transition. For each sample, full diffraction patterns (2θ range 5° – 160°) were collected at 290 and 5 K. The crystal and magnetic structures were then refined with the Rietveld method⁸ using the program FULLPROF.⁹

TABLE I. Unit cell dimensions, atomic positional parameters, and R factors of $(\text{La}_{0.70}\text{Ca}_{0.30})(\text{Cr}_y\text{Mn}_{1-y})\text{O}_3$ at 290 K from Rietveld refinements.

			$y=0.70$	$y=0.50$	$y=0.15$
a (Å)			5.4319(1)	5.4390(2)	5.4571(9)
b (Å)			7.6847(2)	7.6912(3)	7.7162(2)
c (Å)			5.4552(2)	5.4596(3)	5.472(1)
		x	0.0162(4)	0.0188(3)	0.0221(7)
La/Ca	$4c$	y	$\frac{1}{4}$	$\frac{1}{4}$	$\frac{1}{4}$
		z	-0.0031(5)	-0.0046(5)	-0.0087(9)
		x	0	0	0
		y	0	0	0
Cr/Mn	$4b$	z	$\frac{1}{2}$	$\frac{1}{2}$	$\frac{1}{2}$
		x	0.4923(4)	0.4921(1)	0.4939(1)
		y	$\frac{1}{4}$	$\frac{1}{4}$	$\frac{1}{4}$
O_{ax}	$4c$	z	0.0607(4)	0.0617(1)	0.0655(1)
		x	0.2756(3)	0.2753(1)	0.2752(1)
		y	0.0318(2)	0.0316(1)	0.0298(1)
O_{eq}	$8d$	z	0.7258(3)	0.7260(1)	0.7216(1)
R_{Bragg} (%)			5.51	3.68	4.84
R_F (%)			4.95	2.73	3.52

III. RESULTS AND DISCUSSION

In $(\text{La}_{0.70}\text{Ca}_{0.30})\text{MnO}_3$, charge balance imposes a nominal $[\text{Mn}^{3+}]/[\text{Mn}^{4+}]$ ratio equal to 70/30. Upon progressive substitution of Cr^{3+} for Mn, the Mn^{3+} content decreases. The $[\text{Mn}^{3+}]/[\text{Mn}^{4+}]$ ratio becomes 65/35 and 40/60 (for $y=0.15$ and 0.50, respectively), whereas for $y=0.70$ there is no more mixed valence at the B site since all Mn ions are tetravalent. The results of the crystal structure refinement are shown for all samples in Tables I and II at 290 and 5 K, respectively. We observe that the unit cell parameters at both temperatures show a slightly decreasing trend as the Cr content increases. This is consistent with Cr^{3+} substitution which progressively decreases the mean ionic size at the B site [ionic radii are $\text{IR}_{\text{Cr}^{3+}}=0.615$ Å, $\text{IR}_{\text{Mn}^{3+}(\text{HS})}=0.645$ Å, and $\text{IR}_{\text{Mn}^{4+}(\text{HS})}=0.530$ Å].¹⁰

Figure 1 shows the magnetization of the samples at 10 K, as a function of an applied magnetic field. As observed in previous studies,^{5,6} for $y=0.70$ and $y=0.50$ saturation is not achieved even at 12 T, where magnetizations are $\sim 0.15\mu_B$ and $\sim 1.0\mu_B$, respectively, while for $y=0.15$ a saturation magnetization of $\sim 3.10\mu_B$, reached at 3 T, can be assumed. The rising of the saturation field and the decreasing of saturation magnetization with Cr amount suggest that Cr substitution generally hinders FM behavior in $(\text{La}_{0.70}\text{Ca}_{0.30})(\text{Cr}_y\text{Mn}_{1-y})\text{O}_3$.

A. $(\text{La}_{0.70}\text{Ca}_{0.30})(\text{Cr}_{0.70}\text{Mn}_{0.30})\text{O}_3$

A comparison of the NPD data collected at 290 and 5 K shows the onset of an AFM ordering at low temperature. At

the same time, the background is significantly reduced because the incoherent scattering associated with the spin disorder in the PM phase is suppressed. Figure 2 shows the Rietveld refinement plot of the data collected at 5 K; at this temperature a notable contraction of the cell edges is observed. This structural change does not involve a rearrangement of the octahedral tilting, since the O- B -O bond angles are almost coincident with those obtained at 290 K.

$(\text{La}_{0.70}\text{Ca}_{0.30})(\text{Cr}_{0.70}\text{Mn}_{0.30})\text{O}_3$ crystallizes in the $Pnma$ space group at room temperature and retains this structure also at low T . A significant improvement of the fit is obtained by refining the strain parameters. Strain is probably related to the different ionic radii of Cr^{3+} and Mn^{4+} (0.615 and 0.530 Å, respectively),¹⁰ both located at the B site. At 290 K the B atom is located at the center of an almost undistorted octahedron characterized by three very similar B -O bond lengths, whereas at low T a slight distortion is observed which is probably related to the contraction of the cell edges.

The AFM diffraction peaks observed in the NPD pattern at 5 K can be indexed with a propagation vector $\mathbf{k}=0$. Irreducible representation analysis¹¹ yields two possible configurations that are compatible with the experimental AFM G -type structure: Γ_1 (G_x , C_y , A_z) and Γ_5 (A_x , F_y , G_z). An accurate analysis of the NPD data reveals that the magnetic structure belongs to the $Pnma$ Shubnikov space group with the magnetic moments aligned along x (Γ_1). Different magnetic structural models have been tested in order to ascertain if the spins of Cr^{3+} are somehow ordered with those of Mn^{4+} ,

TABLE II. Unit cell dimensions, atomic positional parameters, and R factors of $(\text{La}_{0.70}\text{Ca}_{0.30})(\text{Cr}_y\text{Mn}_{1-y})\text{O}_3$ at 5 K from Rietveld refinements.

			y=0.70	y=0.50	y=0.15
a (Å)			5.4244(1)	5.4324(2)	5.4497(9)
b (Å)			7.6722(2)	7.6808(3)	7.6995(9)
c (Å)			5.4455(1)	5.4505(2)	5.4631(9)
		x	0.0192(3)	0.0211(1)	0.0221(7)
La/Ca	$4c$	y	$\frac{1}{4}$	$\frac{1}{4}$	$\frac{1}{4}$
		z	-0.0048(4)	-0.0054(1)	-0.0080(9)
		x	0	0	0
		y	0	0	0
Cr/Mn	$4b$	z	$\frac{1}{2}$	$\frac{1}{2}$	$\frac{1}{2}$
		x	0.4921(4)	0.4925(1)	0.4943(1)
		y	$\frac{1}{4}$	$\frac{1}{4}$	$\frac{1}{4}$
O_{ax}	$4c$	z	0.0607(3)	0.0633(1)	0.0598(1)
		x	0.2768(2)	0.2763(1)	0.2745(1)
		y	0.0327(2)	0.0321(1)	0.0331(1)
O_{eq}	$8d$	z	0.7253(2)	0.7254(1)	0.72048(1)
R_{Bragg} (%)			4.96	3.99	6.36
R_F (%)			3.95	2.71	4.73

that is, if magnetic interactions take place between Cr^{3+} and Mn^{4+} cations through the intervening O.

Assuming that both ion species take part in the magnetic interactions, we obtain a magnetic moment of $2.22(2)\mu_B$ and R_{magnetic} factor is 2.43%. The refined magnetic moment at the B site is $\sim 70\%$ of the theoretical spin only value ($3.0\mu_B$, from the external electronic configuration t_{2g}^3). This would suggest that only 70% of the magnetic cations are magneti-

cally ordered, a value that matches the amount of substituting Cr^{3+} . Indeed, the best fit result ($R_{\text{magnetic}}=1.99\%$) is obtained assuming that Cr^{3+} are the only cations magnetically ordered. In this case the ordered magnetic moment of Cr^{3+} is equal to $3.20(2)\mu_B$, consistent with the expected theoretical spin only value. Conversely, if only Mn^{4+} are considered with an occupation of 70%, the agreement is somewhat worse ($R_{\text{magnetic}}=3.91\%$). This difference in the R factors reflects the fact that the magnetic form factors of Cr^{3+} and Mn^{4+} are somehow different at wave vectors Q of magnetic interest. This does not *per se* allow any firm conclusion to be drawn on which ionic species takes part in the magnetic order. However, the available magnetization data⁵ suggest clearly that superexchange interactions occur only among neighboring Cr^{3+} cations through the intervening O^2 .

We can then speculate that in $(\text{La}_{0.70}\text{Ca}_{0.30})(\text{Cr}_{0.70}\text{Mn}_{0.30})\text{O}_3$ magnetic interactions between neighboring Cr^{3+} and Mn^{4+} are hindered, although both cations share the same external electronic configuration t_{2g}^3 . In this scenario, Mn^{4+} act as random magnetic impurity in the B sublattice.

The observed magnetic structure is consistent with that detected in $(\text{La}_{1-x}\text{Ca}_x)\text{CrO}_3$ compounds ($x \leq 0.30$). These materials, which are potentially useful for application in solid oxide fuel cells,¹² exhibit a G_x -type spin ordering coupled with a A_z -type one. The magnetic moments increase with the content of calcium, due to the associated increase of Cr^{4+} . Since in $(\text{La}_{0.70}\text{Ca}_{0.30})(\text{Cr}_{0.70}\text{Mn}_{0.30})\text{O}_3$ the whole Cr is

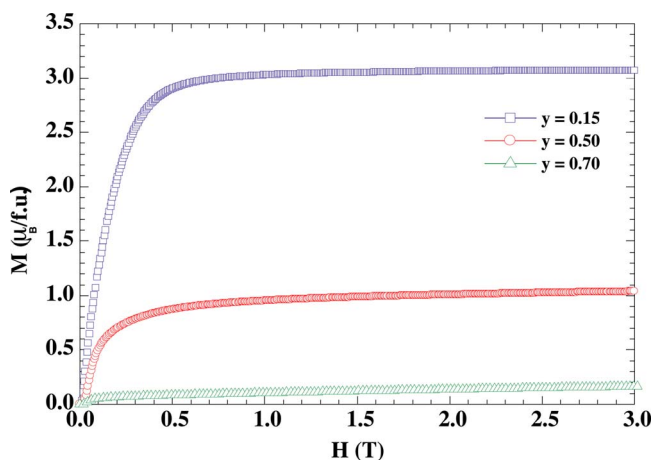


FIG. 1. (Color online) Magnetization as a function of an applied magnetic field in $(\text{La}_{0.70}\text{Ca}_{0.30})(\text{Cr}_y\text{Mn}_{1-y})\text{O}_3$ for $y=0.15, 0.50$, and 0.70 (data collected at 10 K).

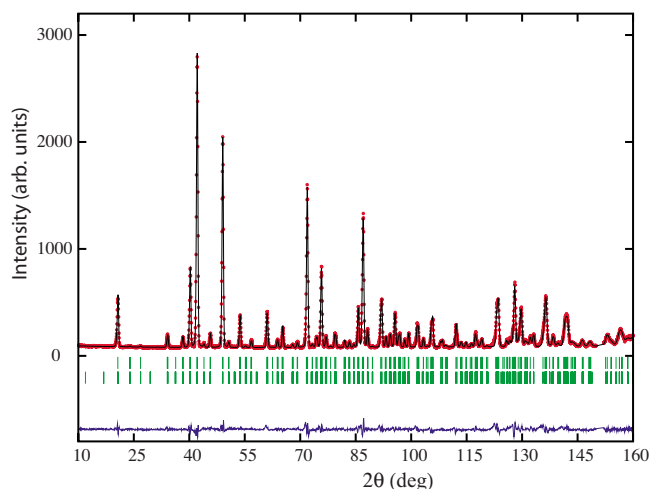


FIG. 2. (Color online) Rietveld refinement plot of the NPD data of $(\text{La}_{0.70}\text{Ca}_{0.30})(\text{Cr}_{0.70}\text{Mn}_{0.30})\text{O}_3$ collected at 5 K on the D2B diffractometer (ILL) with $\lambda=1.5940$ Å. The circles represent the experimental values and the solid line the calculated profile. The upper marks describe the nuclear reflections (the crystal space group is $Pnma$) while the lower set indicates the magnetic ones (antiferromagnetic arrangement G_x). The bottom line is the difference between calculated and experimental profiles.

in the trivalent state, the A_z component is suppressed, as concluded for LaCrO_3 ,¹² where the A_z contribution is extremely faint.

This result is quite intriguing and deserves to be discussed in detail. It is well known that different configurations can contribute to superexchange interactions;^{13,14} in particular, the cation-cation transfer configurations may be more important than others and the overlap integral between the two neighboring cation d orbitals contributes significantly to the exchange integral.¹³ In this context a phenomenological law has been proposed which relates superexchange with the metal-oxygen bond length.¹³ In CaMnO_3 all the manganese ions are Mn^{4+} and their spins order at low T with a G -type magnetic lattice.¹⁵ The same magnetic structure is observed in LaCrO_3 , where all the chromium ions are Cr^{3+} .¹² In CaMnO_3 the Mn^{4+} -O bonds do not exceed 1.90 Å,¹⁵ whereas in LaCrO_3 the Cr^{3+} -O bond length is about 1.95 Å, a value matching that observed in $(\text{La}_{0.70}\text{Ca}_{0.30})(\text{Cr}_{0.70}\text{Mn}_{0.30})\text{O}_3$. Consequently the elongation of the Mn^{4+} -O bond coupled with the reduced size of Mn^{4+} (compared to Cr^{3+}) strongly reduces the overlap between the d orbitals of neighboring Mn^{4+} and Cr^{3+} as well as the superexchange interactions between neighbouring Mn^{4+} . As a result it can be expected that in the B sublattice a Cr^{3+} cation will preferentially interact with neighboring Cr^{3+} and that the Cr^{3+} - Cr^{3+} coupling is favored over the Cr^{3+} - Mn^{4+} one.

The small magnetization measured in saturating conditions is thus consistent with the fact that the AFM ordering of the Cr sublattice is not destroyed by the applied magnetic field, whereas the Mn sublattice can FM order locally.

B. $(\text{La}_{0.70}\text{Ca}_{0.30})(\text{Cr}_{0.50}\text{Mn}_{0.50})\text{O}_3$

The NPD pattern of $(\text{La}_{0.70}\text{Ca}_{0.30})(\text{Cr}_{0.50}\text{Mn}_{0.50})\text{O}_3$ collected at 290 K (Fig. 3) shows an anisotropic asymmetric

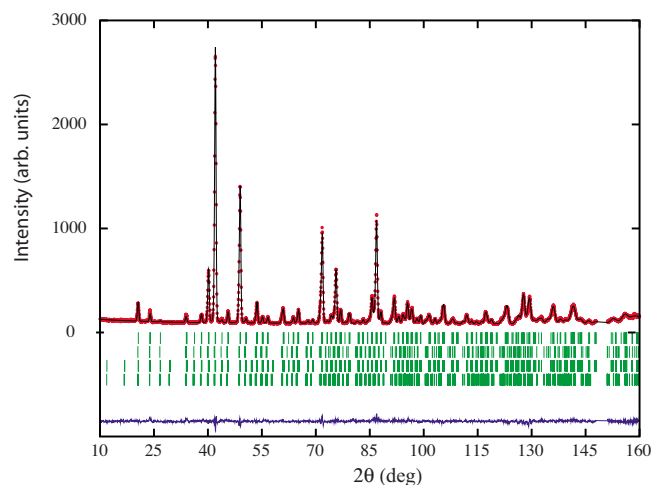


FIG. 3. (Color online) Rietveld refinement plot of the NPD data of $(\text{La}_{0.70}\text{Ca}_{0.30})(\text{Cr}_{0.50}\text{Mn}_{0.50})\text{O}_3$ collected at 5 K on the D2B diffractometer (ILL) with $\lambda=1.5940$ Å. The experimental data (circles) are better described by two isostructural phases (two upper sets of marks). The two lower sets are the magnetic reflections of the two nuclear phases. The bottom line is the difference between calculated (solid line) and experimental profiles. The crystal space is $Pnma$ and the magnetic structures are antiferromagnetic of type G_x .

line broadening of the diffraction peaks. The single nominal phase yields a reasonable fit. However, a notable improvement of the R factors and fitting profile is obtained assuming the coexistence of two different isostructural phases characterized by slightly different $[\text{Mn}]/[\text{Cr}]$ ratios. The inhomogeneous distribution of Mn and Cr could be due to an incipient phase separation, occurred during the cooling stage of the sample preparation, or to an incompleteness of the reaction. According to our Rietveld refinement, the main phase constitutes about 86% of the total molar content and is characterized by a $[\text{Mn}]/[\text{Cr}]$ ratio equal to ~ 1.20 , a value quite close to the nominal one (1.00). The lattice and structural parameters of this phase are reported in Tables I and II. The secondary phase is probably better described by a mixture of Cr-enriched isostructural phases exhibiting slight variations of the $[\text{Mn}]/[\text{Cr}]$ ratio. In any case this sample gives a clear indication of how Mn and Cr behave when they share the same atomic site with about the same degree of occupancy. The NPD pattern at 5 K shows the same AFM peaks (G type) observed in the sample $(\text{La}_{0.70}\text{Ca}_{0.30})(\text{Cr}_{0.70}\text{Mn}_{0.30})\text{O}_3$, although their intensities are decreased (Fig. 4). Since Cr is known to destroy AFM ordering in the Mn sublattice of manganites, this suggests that this peak arise from an AFM structure occurring in the Cr sublattice. Note that the peak at $2\theta \sim 24^\circ$ in Fig. 4 is due to the nuclear structure for $y=0.50$ (it is observed also in the NPD pattern collected at 290 K), whereas it has a magnetic origin in the sample with $y=0.15$.

Small angle neutron scattering (SANS) is essentially the same at 290 and 5 K. In manganites SANS contribution is related to the development of FM clusters in the PM region¹⁶ and the onset of a long-range magnetic order suppresses this contribution. In $(\text{La}_{0.70}\text{Ca}_{0.30})(\text{Cr}_{0.50}\text{Mn}_{0.50})\text{O}_3$ the presence

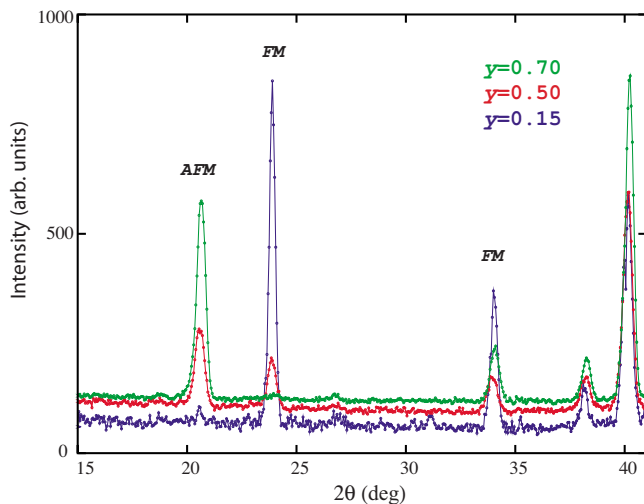


FIG. 4. (Color online) Low-angle portion of the NPD patterns of $(\text{La}_{0.70}\text{Ca}_{0.30})(\text{Cr}_y\text{Mn}_{1-y})\text{O}_3$ collected at 5 K. The intensity of the AFM peak decreases progressively upon increasing y from 0.70 to 0.50, and it vanishes for $y=0.15$. The sample with $y=0.15$ conversely shows only FM peaks (a weak nuclear contribution is present at $2\theta \sim 21.5^\circ$).

of SANS at low T is probably related to the fact that long-range magnetic order does not take place in the Mn sublattice at low T and hence FM clusters do not percolate on cooling. A similar behavior characterizes also the $(\text{La}_{0.70}\text{Ca}_{0.30})(\text{Cr}_{0.70}\text{Mn}_{0.30})\text{O}_3$ sample, although in this case it is partially masked by the evolution of the incoherent scattering with T . Contrary, in $(\text{La}_{0.70}\text{Ca}_{0.30})(\text{Cr}_{0.50}\text{Mn}_{0.50})\text{O}_3$ the incoherent scattering exhibits a faint decrease with T because it is dominated not by spin disorder as in the previous case but by chemical disorder at the B site.

The magnetization under saturation of this sample is consistent with the scenario already proposed for $(\text{La}_{0.70}\text{Ca}_{0.30})(\text{Cr}_{0.70}\text{Mn}_{0.30})\text{O}_3$, where the applied magnetic field does not destroy the AFM ordering of the Cr sublattice, but aligns ferromagnetically a fraction of the Mn spins.

In the Rietveld refinement, several models have been tested for the magnetic structure. In particular, the addition of a ferromagnetic component does not improve the R factors and yields a FM moment which is too small to have physical significance. We therefore conclude that this Cr concentration is characterized by the same magnetic structure as $(\text{La}_{0.70}\text{Ca}_{0.30})(\text{Cr}_{0.70}\text{Mn}_{0.30})\text{O}_3$ with an AFM moment on the Cr ions equal to $2.40(1)\mu_B$.

C. $(\text{La}_{0.70}\text{Ca}_{0.30})(\text{Cr}_{0.15}\text{Mn}_{0.85})\text{O}_3$

For this chromium concentration, saturation is reached at 3 T and the magnetization is $\sim 3.10\mu_B$; this value matches exactly what is expected considering only the Mn sublattice FM ordered. If both Mn and Cr cations are considered FM aligned the resulting nominal moment is $3.55\mu_B$, a value which exceeds by far the experimental one. This suggests that Cr^{3+} does not participate in the mechanism of double exchange that takes place between the Mn^{3+} and Mn^{4+} cations and leads to the onset of the FM spin order. We have

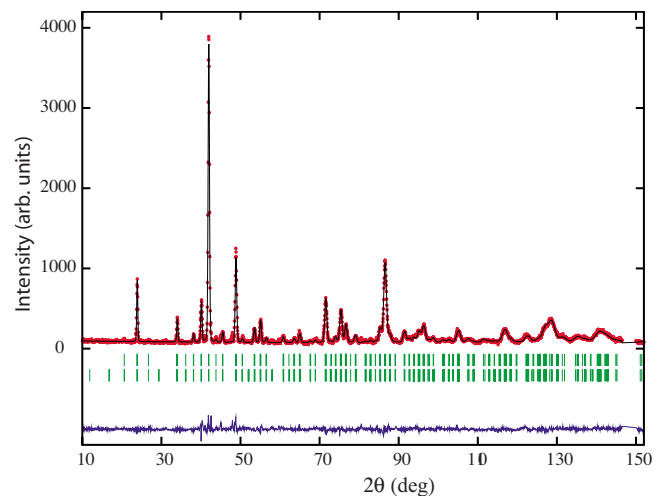


FIG. 5. (Color online) Rietveld refinement plot of the NPD data of $(\text{La}_{0.70}\text{Ca}_{0.30})(\text{Cr}_{0.15}\text{Mn}_{0.85})\text{O}_3$ collected at 5 K on the D2B diffractometer (ILL) with $\lambda = 1.5940 \text{ \AA}$. The upper marks describe the nuclear reflections (SG $Pnma$) while the lower set corresponds to the magnetic one (ferromagnetic type with the spins aligned along z). The bottom line is the difference between calculated (solid line) and experimental profiles (circles).

once again tested several magnetic models using the Rietveld method in order to determine what cationic species are FM ordered. The best agreement (Fig. 5) is obtained assuming that only the Mn ions are FM ordered along the z axis, whereas Cr^{3+} ions act as random impurities. The value of the Mn spin is found to be $2.90(4)\mu_B$.

Our analysis gives strong microscopic evidence of what has been suggested on the basis of magnetization and resistivity measurements,^{5,6} i.e., that conducting electrons participating in the double exchange do not interact with Cr^{3+} . As a consequence Cr^{3+} ions are not magnetically ordered but their spins are randomly oriented within the B sublattice.

Unlike what observed in $(\text{La}_{0.70}\text{Ca}_{0.30})(\text{Cr}_{0.5}\text{Mn}_{0.5})\text{O}_3$, at this chromium concentration, the NPD data do show a decrease of SANS contribution with decreasing T . This is consistent with a percolation of FM clusters below the Curie temperature. At the same time incoherent scattering is partially suppressed on cooling and the background is decreased.

IV. CONCLUSIONS

The nuclear and magnetic structures of $(\text{La}_{0.70}\text{Ca}_{0.30})(\text{Cr}_y\text{Mn}_{1-y})\text{O}_3$ samples ($y=0.70, 0.50$, and 0.15) at 290 and 5 K have been investigated by means of neutron powder diffraction. For samples with $y=0.70$ and 0.50 an AFM structure (G_x type) occurs in the Cr sublattice at 5 K, whereas the spins of the Mn ions are randomly oriented. The sample with $y=0.15$ exhibits FM ordering of the Mn spins at 5 K while Cr is not involved in the double exchange. In conclusion no evidence for double or superexchange interactions among Cr^{3+} and Mn cationic species has been observed. In particular, it has been found that superexchange interactions among Cr^{3+} ions prevail for $y=0.70, 0.50$,

whereas for $y=0.15$ double exchange takes place among Mn cationic species only.

ACKNOWLEDGMENTS

We acknowledge the School of Chemistry and the School

of Physics and Astronomy of the University of Birmingham, the EPSRC (UK), and the EC (Training and Mobility of Researchers) for supporting part of this work. We thank L. Chapon for useful discussions during the International School of Neutron Scattering F. P. Ricci (Sardinia 2006).

-
- ¹J. B. Goodenough, *Phys. Rev.* **100**, 564 (1955).
²E. O. Wollan and W. C. Koehler, *Phys. Rev.* **100**, 545 (1955).
³B. Raveau, A. Maignan, C. Martin, and M. Hervieu, *Chem. Mater.* **10**, 2641 (1998).
⁴A. J. Millis, R. Mueller, and B. I. Shraiman, *Phys. Rev. B* **54**, 5389 (1996).
⁵O. Cabeza, M. Long, C. Severac, M. A. Bari, C. M. Muirhead, M. G. Francesconi, and C. Greaves, *J. Phys.: Condens. Matter* **11**, 2569 (1999).
⁶O. Cabeza, O. Barca, G. Francesconi, M. A. Bari, C. Severack, C. M. Muirhead, and F. Miguélez, *J. Magn. Magn. Mater.* **196-197**, 504 (1999).
⁷B. Raveau, A. Maignan, and C. Martin, *J. Solid State Chem.* **130**, 162 (1997).
⁸R. A. Young, *The Rietveld Method*, IUCr Monographs on Crystallography Vol. 5 (Oxford University Press, Oxford, 1993), Chap. 1, pp. 1–38.
⁹J. Rodríguez-Carvajal, *Physica B* **192**, 55 (1993).
¹⁰R. D. Shannon, *Acta Crystallogr., Sect. A: Cryst. Phys., Diffr., Theor. Gen. Crystallogr.* **32**, 751 (1976).
¹¹E. F. Bertaut, *Acta Crystallogr., Sect. A: Cryst. Phys., Diffr., Theor. Gen. Crystallogr.* **24**, 217 (1968).
¹²N. Sakai, H. Fjellvåg, and B. C. Hauback, *J. Solid State Chem.* **121**, 202 (1996).
¹³Nai Li Huang and R. Orbach, *Phys. Rev.* **154**, 487 (1967).
¹⁴Keshav N. Shrivastava and V. Jaccarino, *Phys. Rev. B* **13**, 299 (1976).
¹⁵K. R. Poeppelmeier, M. E. Leonowicz, J. C. Scanlon, J. M. Longo, and W. B. Yelon, *J. Solid State Chem.* **45**, 71 (1982).
¹⁶J. M. De Teresa, M. R. Ibarra, J. Blasco, J. García, C. Marquina, P. A. Algarabel, Z. Arnold, K. Kamenev, C. Ritter, and R. von Helmolt, *Phys. Rev. B* **54**, 1187 (1996).